

# Dynamical Properties of an Antiferromagnet near the Quantum Critical Point: Application to $\text{LaCuO}_{2.5}$

B. Normand and T. M. Rice

*Theoretische Physik, ETH-Hönggerberg, CH-8093 Zürich, Switzerland.*

(June 26, 2018)

## Abstract

For a system of two-chain spin ladders, the ground state for weak interladder coupling is the spin-liquid state of the isolated ladder, but is an ordered antiferromagnet (AF) for sufficiently large interactions. We generalize the bond-operator mean-field theory to describe both regimes, and to focus on the transition between them. In the AF phase near the quantum critical point (QCP) we find both spin waves and a low-lying but massive amplitude mode which is absent in a conventional AF. The static susceptibility has the form  $\chi(T) = \chi_0 + aT^2$ , with  $\chi_0$  small for a system near criticality. We consider the dynamical properties to examine novel features due to the presence of the amplitude mode, and compute the dynamic structure factor.  $\text{LaCuO}_{2.5}$  is thought to be such an unconventional AF, whose ordered phase is located very close to the QCP of the transition to the spin liquid. From the Néel temperature we deduce the interladder coupling, the small ordered moment and the gap in the amplitude mode. The dynamical properties unique to near-critical AFs are expected to be observable in  $\text{LaCuO}_{2.5}$ .

PACS numbers: 75.10.Jm, 75.30.Kz, 75.40.Cx, 75.50.Ee

Typeset using REVTeX

## I. INTRODUCTION

The study of spin ladder systems [1] has made rapid progress since their synthesis [2] and identification. [3] Among the problems investigated both theoretically and experimentally are the nature of the ground state, which is dramatically different for ladders composed of odd and even numbers of chains, the behavior of holes in ladders, including their superconductivity, [4] and the properties introduced by doping of spinless impurities. Further novel physical phenomena are found in coupled spin ladders, where the magnetic structure of even-chain ladders with unfrustrated coupling, is of particular interest because the ground state is expected to be a spin liquid at sufficiently weak coupling, but to order magnetically when the interladder interactions are strong. This system realizes the conditions required to investigate the QCP, introduced by Chakravarty *et al.* [5] in the context of a nonlinear  $\sigma$ -model description of the two-dimensional Heisenberg AF, and discussed extensively and more generally in Refs. [6] and [7]. In the language of these analyses, the interladder coupling is a parameter which tunes the system from the renormalized classical regime of long-ranged magnetic order, through the QCP to the one-dimensional limit where the spins are disordered by quantum fluctuations (quantum disordered).

Such a structure is represented in three dimensions by the two-chain ladder compound  $\text{LaCuO}_{2.5}$ . [8] Initial experimental studies gave contradictory results on the nature of the ground state, as static susceptibility measurements [8] suggested a spin liquid state with a spin gap, while nuclear magnetic resonance (NMR) [9] and muon spin resonance ( $\mu\text{SR}$ ) [10] measurements indicated a transition to a magnetically ordered phase. In a brief study of both electronic and magnetic properties of the material, it was proposed [11] that the conflicting observations could be reconciled if the system was located near the QCP of the transition between the two regimes, and this scenario was supported by detailed numerical simulations performed by Troyer *et al.* [12]

In this work we will analyze the properties of the system on both sides of the critical point, employing a mean-field approximation to the bond-operator technique which is generalized

to the magnetically ordered regime. From the evolution of the mode structure through the transition, we may compute both the thermodynamics and the dynamical magnetic properties of the system. In the disordered phase, the excitations are triply degenerate magnons with a spin gap which vanishes on approach to the QCP. In the AF ordered phase, we find that the modes evolve into two spin-wave excitations representing rotations of the ordered moment, accompanied by an amplitude mode corresponding to fluctuations in its magnitude. This latter mode has a gap which grows continuously with the moment, so it will be low-lying only near the QCP, and will develop far from the transition into a high-lying excitation which is ignored in the dynamics of a conventional AF.

To characterize the ordered system close to the QCP we focus on the static susceptibility  $\chi(T)$ , which vanishes at  $T = 0$  on approach to the transition. The results for  $\chi(T)$  in the mean-field theory agree well both qualitatively and quantitatively by highly accurate Quantum Monte Carlo studies carried out by Troyer *et al.* [12] Both sets of calculations support the proposal that  $\text{LaCuO}_{2.5}$  is indeed an AF close to the QCP.

We examine the dynamic structure factor to find features associated with the presence of an amplitude mode. This mode couples to neutrons in the same way as the transverse excitations, and we show that it should be observable in inelastic neutron scattering measurements on single crystals. Raman light scattering by the magnetic excitations is also discussed, but in this case it is difficult to find signals which may be ascribed unambiguously to this mode.

The outline of this paper is as follows. In section II we develop the bond-operator formalism for application in the ordered magnetic regime, to describe the mode structure of the magnetic excitations and the zero-temperature phase transition. In section III we discuss briefly the statistics of the magnon excitations, in order to solve the mean-field equations at finite temperatures and to deduce the static susceptibility on both sides of the transition. We consider in section IV the dynamical magnetic properties of the system in the vicinity of the QCP, and calculate the dynamic structure factor for comparison with proposed experiments. Section V contains our conclusions and a brief discussion.

## II. ORDERED MAGNETIC PHASE

We begin by applying the bond-operator technique [13,14] in the regime where the interladder superexchange coupling is sufficiently strong to stabilize a magnetically ordered state. We will restrict ourselves to the case of simple AF order both along and perpendicular to the ladders. However, we shall return in section IV to a recent alternative proposition, and show that this gives rise only to notational differences.

Following Ref. [13], the spin degrees of freedom on each ladder rung are represented by the bond operators

$$\begin{aligned} |s\rangle &= s^\dagger|0\rangle = \frac{1}{\sqrt{2}}(|\uparrow\downarrow\rangle - |\downarrow\uparrow\rangle), \\ |t_x\rangle &= t_x^\dagger|0\rangle = -\frac{1}{\sqrt{2}}(|\uparrow\uparrow\rangle - |\downarrow\downarrow\rangle), \\ |t_y\rangle &= t_y^\dagger|0\rangle = \frac{i}{\sqrt{2}}(|\uparrow\uparrow\rangle + |\downarrow\downarrow\rangle), \\ |t_z\rangle &= t_z^\dagger|0\rangle = \frac{1}{\sqrt{2}}(|\uparrow\downarrow\rangle + |\downarrow\uparrow\rangle), \end{aligned} \tag{1}$$

where the arrows denote the direction of the left and right spins. The presence of a quadratic term with negative coefficient in the transformed Heisenberg Hamiltonian ensures that the singlet operators condense, so that one may take  $\langle s_i \rangle = \bar{s}$  on each rung. AF ordering along the ladders occurs when, in addition, one of the triplet operators has a non-zero expectation value with alternating sign. This we take to be the component  $t_z$ , which may be written as

$$t_{iz} = (-1)^{iz} \bar{t} + \hat{t}_{iz}, \tag{2}$$

where  $\hat{t}_z$  contains fluctuations about the average value  $\bar{t}$ . The dynamics of these fluctuations may not be neglected, as in the treatment of the  $s$  degree of freedom, because their dispersion is strong. With this choice of basis states, the coexistence of a finite  $\bar{t}$  with the condensed singlet  $\bar{s}$  on a rung corresponds to an AF alternation along the ladder of states  $|\uparrow\downarrow\rangle$  and  $|\downarrow\uparrow\rangle$  of fixed, staggered moment  $\bar{t}$ , admixed with a singlet component of weight  $\bar{s} - \bar{t}$ .

In the disordered or spin-liquid regime the three triplet modes remain degenerate and massive, a situation represented schematically in Fig. 1(a). The spin gap vanishes as the

coupling approaches the QCP, where the three modes of the lower branch are spin-wave-like, with a linear dispersion about the wave vector of the magnetic ordering (Fig. 1(b)). In AF the ordered phase there is a spontaneous breaking of rotational symmetry, which by Goldstone's theorem is accompanied by massless excitations. These will be two spin waves, which represent rotations, or transverse oscillations, of the finite staggered moment. The third mode corresponds to fluctuations in the amplitude of the moment (longitudinal) and will acquire a finite gap, as shown in Fig. 1(c). In a conventional AF system one observes only the two spin waves, but close to the QCP the amplitude mode will also be of low energy at the zone center.

The real-space axes, not to be confused with spin-space labels introduced above, are chosen with  $\hat{\mathbf{z}}$  along the ladder direction and  $\hat{\mathbf{x}}$  and  $\hat{\mathbf{y}}$  the directions of interladder coupling. Using the reduced unit cell [12] in the  $x$ - and  $y$ -dimensions, but with doubling of the real-space structure in the  $z$ -direction to accommodate AF ordering along the ladder, the Hamiltonian of the three-dimensionally coupled system,

$$H = J \sum_j \mathbf{S}_{l,j} \cdot \mathbf{S}_{r,j} + \lambda J \sum_{j,m=l,r} \mathbf{S}_{m,j} \cdot \mathbf{S}_{m,j+\hat{z}} + \lambda' J \sum_j (\mathbf{S}_{r,j} \cdot \mathbf{S}_{l,j+\hat{x}} + \mathbf{S}_{r,j} \cdot \mathbf{S}_{l,j+\hat{y}}), \quad (3)$$

after transformation to bond operators is written as

$$H = H_0 + H_1 + H_2 + H_3 + H_4, \quad (4)$$

where the terms have the following origins.

$$H_0 = J \sum_{j,\alpha} \sum_{m=1,2} \left( -\frac{3}{4} s_j^{m\dagger} s_j^m + \frac{1}{4} t_{j,\alpha}^{m\dagger} t_{j,\alpha}^m \right) - \sum_{j,\alpha} \sum_{m=1,2} \mu_{j,m} \left( s_j^{m\dagger} s_j^m + t_{j,\alpha}^{m\dagger} t_{j,\alpha}^m - 1 \right) \quad (5)$$

contains the contribution from the ladder rung interactions, and also the constraint which restricts the spin states on each rung to a singlet or one of three triplets. Here  $j$  is a unit cell index and  $m$  an index for the two types of rung in each cell.

$$H_1 = \frac{1}{2}\lambda J \sum_{j,\alpha} \sum_{m=1,2} \left( t_{j,\alpha}^{m\dagger} t_{j+\hat{z},\alpha}^{m+1\dagger} s_j^{m+1} s_j^m + t_{j,\alpha}^{m\dagger} t_{j+\hat{z},\alpha}^{m+1\dagger} s_j^m s_{j+\hat{z}}^{m+1} + H.c. \right) \quad (6)$$

and

$$H_2 = \frac{1}{4}\lambda J \sum_{j,\alpha \neq \beta} \sum_{m=1,2} \left( t_{j,\alpha}^{m\dagger} t_{j+\hat{z},\beta}^{m+1\dagger} t_{j+\hat{z},\alpha}^{m+1} t_{j,\beta}^m - t_{j,\alpha}^{m\dagger} t_{j+\hat{z},\alpha}^{m+1\dagger} t_{j+\hat{z},\beta}^{m+1} t_{j,\beta}^m + H.c. \right) \quad (7)$$

are the terms quadratic and quartic in  $t$  operators corresponding to ladder leg interactions;  $H_2$  may not be discarded in the ordered system because it will contribute terms of order  $\bar{t}^2$  to the dynamics of the modes  $\alpha = x, y$ .

$$H_3 = -\frac{1}{4}\lambda' J \sum_{j,\alpha} \sum_{\eta=\pm\hat{x},\hat{y}} \sum_{m=1,2} \left( t_{j,\alpha}^{m\dagger} t_{j+\eta,\alpha}^m s_{j+\eta}^{m\dagger} s_j^m + t_{j,\alpha}^{m\dagger} t_{j+\eta,\alpha}^{m\dagger} s_{j+\eta}^m s_j^m + H.c. \right) \quad (8)$$

and

$$H_4 = \frac{1}{8}\lambda' J \sum_{j,\alpha} \sum_{\eta=\pm\hat{x},\hat{y}} \sum_{m=1,2} \left( t_{j,\alpha}^{m\dagger} t_{j+\eta,\beta}^{m\dagger} t_{j+\eta,\alpha}^m t_{j,\beta}^m - t_{j,\alpha}^{m\dagger} t_{j+\eta,\alpha}^{m\dagger} t_{j+\eta,\beta}^m t_{j,\beta}^m + H.c. \right) \quad (9)$$

are the quadratic and quartic contributions from the interladder coupling terms, which link rungs of the same type  $m$ .

In the mean-field approximation the singlet expectation value  $\langle s_i^m \rangle = \bar{s}$  and Lagrange multiplier  $\mu_i^m = \mu$  are taken to be the same on all rungs  $(i, m)$ , while the triplet expectation value  $\langle t_{i,z}^m \rangle = -(-1)^m \bar{t}$  alternates. The constraint term incorporates a reduction of  $\bar{s}$  due both to the presence of the  $\bar{t}$  term and to quadratic fluctuations of all three magnon modes. A direct coupling of the longitudinal ( $t_z$ ) fluctuations to the magnitude of  $\bar{s}$  is also relevant, and appears in the  $t_z^\dagger t_z s^\dagger s$  terms as

$$\begin{aligned} t_{j,z}^\dagger t_{j+\hat{z},z} s_j^\dagger s_j &= t_{j,z}^\dagger t_{j+\hat{z},z} \left( 1 - t_{j,z}^\dagger t_{j,z} \right)^{1/2} \left( 1 - t_{j+\hat{z},z}^\dagger t_{j+\hat{z},z} \right)^{1/2} \\ &\simeq (\bar{t} + \hat{t}_{j,z}^\dagger)(-\bar{t} + \hat{t}_{j+\hat{z},z}) \left( \bar{s} - \frac{1}{2\bar{s}} \hat{t}_{j,z}^\dagger \hat{t}_{j,z} \right) \left( \bar{s} - \frac{1}{2\bar{s}} \hat{t}_{j+\hat{z},z}^\dagger \hat{t}_{j+\hat{z},z} \right) \\ &= -\bar{s}^2 \bar{t}^2 + \bar{s}^2 \hat{t}_{j,z}^\dagger \hat{t}_{j+\hat{z},z} + \frac{1}{2} \bar{t}^2 \left( \hat{t}_{j,z}^\dagger \hat{t}_{j,z} + \hat{t}_{j+\hat{z},z}^\dagger \hat{t}_{j+\hat{z},z} \right) + O(\hat{t}^4). \end{aligned} \quad (10)$$

The first line follows from substitution of the number operators into the constraint and the second from Eq. (2). In the last line, the first term is the classical part, the second is a

fluctuation term which will appear in off-diagonal components of the Hamiltonian matrix for all leg and interrung coupling combinations in  $H$  and for all three polarizations  $\hat{t}_\alpha$ , and the third is diagonal in the magnon operators so appears as a mass term unique to the  $t_z$  modes. Note that the mass grows with the ordered moment  $\bar{t}$ , as would be expected.

The mean-field Hamiltonian in reciprocal space may be cast in the form

$$\begin{aligned}
H_m(\mu, \bar{s}, \bar{t}) = N & \left( -\frac{3}{4}J\bar{s}^2 + \frac{1}{4}J\bar{t}^2 - \mu\bar{s}^2 - \mu\bar{t}^2 + \mu - 2J\bar{s}^2\bar{t}^2(\lambda + \lambda') \right) \\
& + \sum_{\mathbf{k}\alpha} \left\{ \sum_{m=1,2} \left[ \Lambda_{\mathbf{k}}^\alpha t_{\mathbf{k}\alpha}^{m\dagger} t_{\mathbf{k}\alpha}^m + \Delta_{\mathbf{k}}^\alpha \left( t_{\mathbf{k}\alpha}^{m\dagger} t_{-\mathbf{k}\alpha}^{m\dagger} + t_{\mathbf{k}\alpha}^m t_{-\mathbf{k}\alpha}^m \right) \right] \right. \\
& \left. + \left[ \Lambda_{\mathbf{k}}^{\prime\alpha} t_{\mathbf{k}\alpha}^{1\dagger} t_{\mathbf{k}\alpha}^2 + \Delta_{\mathbf{k}}^{\prime\alpha} \left( t_{\mathbf{k}\alpha}^{1\dagger} t_{-\mathbf{k}\alpha}^{2\dagger} + t_{\mathbf{k}\alpha}^1 t_{-\mathbf{k}\alpha}^2 \right) \right] + [1 \leftrightarrow 2] \right\},
\end{aligned} \tag{11}$$

in which  $N$  denotes the total number of ladder rungs, the coefficients for the transverse modes  $\alpha = \sigma \equiv (x, y)$  are

$$\Lambda_{\mathbf{k}}^\sigma = \frac{1}{4}J - \mu - \frac{1}{2}\lambda'J(\bar{s}^2 - \bar{t}^2)(\cos k_x + \cos k_y), \tag{12}$$

$$\Delta_{\mathbf{k}}^\sigma = \frac{1}{4}\lambda'J(\bar{s}^2 + \bar{t}^2)(\cos k_x + \cos k_y), \tag{13}$$

$$\Lambda_{\mathbf{k}}^{\prime\sigma} = J(\bar{s}^2 - \bar{t}^2) \cos \frac{1}{2}k_z \tag{14}$$

and

$$\Delta_{\mathbf{k}}^{\prime\sigma} = \frac{1}{2}J(\bar{s}^2 + \bar{t}^2) \cos \frac{1}{2}k_z, \tag{15}$$

and for the amplitude modes  $\alpha = z$ ,

$$\Lambda_{\mathbf{k}}^z = \frac{1}{4}J - \mu + 2J\bar{t}^2(\lambda + \lambda') - \frac{1}{2}\lambda'J\bar{s}^2(\cos k_x + \cos k_y), \tag{16}$$

$$\Delta_{\mathbf{k}}^z = \frac{1}{4}\lambda'J\bar{s}^2(\cos k_x + \cos k_y), \tag{17}$$

and

$$\Lambda_{\mathbf{k}}^{\prime z} = 2\Delta_{\mathbf{k}}^{\prime z} = \frac{1}{2}J\bar{s}^2 \cos \frac{1}{2}k_z. \tag{18}$$

The part of  $H_m$  (11) quadratic in the triplet operators is diagonalized by Bogoliubov transformation, and can be reexpressed in terms of the appropriate quasiparticle operators  $\gamma_{k\alpha}^\pm$  as

$$H_m(\mu, \bar{s}, \bar{t}) = N \left( -\frac{3}{4}J\bar{s}^2 + \frac{1}{4}J\bar{t}^2 - \mu\bar{s}^2 - \mu\bar{t}^2 + \mu - 2J\bar{s}^2\bar{t}^2(\lambda + \lambda') \right) - N \left( \frac{1}{4}J - \mu \right) - \frac{1}{2}N \left( \frac{1}{4}J - \mu + 2J\bar{t}^2(\lambda + \lambda') \right) \quad (19)$$

$$+ \sum_{\mathbf{k}\alpha} \sum_{\nu=\pm} \omega_{\mathbf{k}\alpha}^\nu \left( \gamma_{\mathbf{k}\alpha}^{\nu\dagger} \gamma_{\mathbf{k}\alpha}^\nu + \frac{1}{2} \right). \quad (20)$$

In calculating the mode frequencies, all terms fourth order in  $\bar{s}$  and  $\bar{t}$  are found to cancel, giving the easily factorized results

$$\omega_{\mathbf{k}\sigma}^\nu = \left[ \left( \frac{1}{4}J - \mu - 2\nu J\bar{s}^2 a_{\mathbf{k}}^\nu \right) \left( \frac{1}{4}J - \mu + 2\nu J\bar{t}^2 a_{\mathbf{k}}^\nu \right) \right]^{1/2} \quad (21)$$

and

$$\omega_{\mathbf{k}z}^\nu = \left[ \left( \frac{1}{4}J - \mu + 2J\bar{t}^2(\lambda + \lambda') \right) \left( \frac{1}{4}J - \mu + 2J\bar{t}^2(\lambda + \lambda') - 2\nu J\bar{s}^2 a_{\mathbf{k}}^\nu \right) \right]^{1/2}, \quad (22)$$

where

$$a_{\mathbf{k}}^\pm = \lambda \cos \frac{1}{2}k_z \pm \frac{1}{2}\lambda'(\cos k_x + \cos k_y). \quad (23)$$

The equation for  $\omega_{\mathbf{k}z}^\pm$  represents two branches for the amplitude mode in the doubled Brillouin zone; folding back of the zone in the  $k_x$  and  $k_y$  dimensions returns the four branches in the Brillouin zone of the real material. The equation for  $\omega_{\mathbf{k}\sigma}^\pm$  contains four doubly-degenerate branches, of which the most interesting is the lowest-lying,  $\omega_{\mathbf{k}\sigma}^+$  with  $k_x$  and  $k_y$  in the reduced Brillouin zone. This yields the two rotation modes, and from the factorized form (21) it is clear that the spin-wave condition is the same as the vanishing of the spin gap which gave the critical coupling for the transition from the disordered side,  $\frac{1}{4}J - \mu = 2J\bar{s}^2(\lambda + \lambda')$ .

That the massless modes described by the bond operators are indeed true spin waves can be shown in two ways. First, considering the limit of fully developed magnetic order,  $\bar{s} = \bar{t} = \frac{1}{\sqrt{2}}$  and



$$\begin{aligned}\omega_{\mathbf{k}\sigma}^+ &= \left(\frac{1}{4}J - \mu\right) \left[1 - \left(\frac{a_{\mathbf{k}}^{+2}}{\lambda + \lambda'}\right)^2\right]^{1/2} \\ &\simeq 2J\bar{s}^2 \sqrt{(\lambda + \lambda')} \left[\frac{1}{4}\lambda k_z^2 + \frac{1}{2}(k_x^2 + k_y^2)\right]^{1/2}\end{aligned}\quad (24)$$

in the limit of small  $k$ . A textbook derivation [15] of the mode spectrum for the Hamiltonian in Eq. (3), for a spins of arbitrary magnitude  $S$  and with four spins per unit cell, returns exactly the contents of both lines in Eq. (24), with the condition  $S = \bar{s}^2 = \frac{1}{2}$ , as required. More generally, in the spin basis of Eq. (1) it is straightforward to show that a spin wave, represented by a staggered, transverse component of  $S_x$  on each rung, may be represented by the bond-operator states  $-|t_x\rangle - |s\rangle$ , and similarly for  $S_y$ , showing its equivalence to a  $t_x$  ( $t_y$ ) bond-operator mode in the presence of the singlet.

The average singlet and triplet occupations may be represented by the reduced variables

$$d_s = \frac{2J\bar{s}^2}{\frac{1}{4}J - \mu} \quad d_t = \frac{2J\bar{t}^2}{\frac{1}{4}J - \mu}, \quad (25)$$

in terms of which the mode frequencies (21) and (22) are given by

$$\omega_{\mathbf{k}\sigma}^\nu = \left(\frac{1}{4}J - \mu\right) \sqrt{(1 - \nu d_s a_k^\nu)(1 + \nu d_t a_k^\nu)} \quad (26)$$

and

$$\omega_{\mathbf{k}z}^\nu = \left(\frac{1}{4}J - \mu\right) \sqrt{(1 + d_t(\lambda + \lambda'))(1 + d_t(\lambda + \lambda') - \nu d_s a_k^\nu)}, \quad (27)$$

while the spin-wave condition, which is maintained everywhere in the ordered regime, becomes

$$d_s = (\lambda + \lambda')^{-1}. \quad (28)$$

By substitution into the self-consistency equation for the disordered solution, [11] the critical coupling  $\lambda'_c$  is given implicitly by

$$\frac{1}{\lambda + \lambda'_c} = 5 - 3 \sum_k' \left(1 + \frac{a_k}{\lambda + \lambda'_c}\right)^{-1/2} n_m(\omega_{\mathbf{k}}), \quad (29)$$

where in the reduced unit cell there is only one degenerate magnon branch. In the remainder of this section we will consider the system at zero temperature, so that the magnon thermal occupation factors  $n_m(\omega_{\mathbf{k}}^\nu)$  are unity. The full mean-field equations are

$$\begin{aligned} \left\langle \frac{\partial H_m}{\partial \mu} \right\rangle = 0 = & -\bar{s}^2 - \bar{t}^2 + 1 \\ & + \frac{3}{2} - \frac{1}{2} \sum'_{\mathbf{k}\nu} \frac{1 + d_t(\lambda + \lambda') - \frac{1}{2}\nu d_s a_{\mathbf{k}}^\nu}{2\sqrt{(1 + d_t(\lambda + \lambda'))(1 + d_t(\lambda + \lambda') - \nu d_s a_{\mathbf{k}}^\nu)}} \\ & - \sum'_{\mathbf{k}\nu} \frac{1 + \frac{1}{2}\nu d_t a_{\mathbf{k}}^\nu - \frac{1}{2}\nu d_s a_{\mathbf{k}}^\nu}{2\sqrt{(1 - \nu d_s a_{\mathbf{k}}^\nu)(1 + \nu d_t a_{\mathbf{k}}^\nu)}} \end{aligned} \quad (30)$$

$$\begin{aligned} \left\langle \frac{\partial H_m}{\partial \bar{s}} \right\rangle = 0 = & -\frac{3}{4}J - \mu - 2J\bar{t}^2(\lambda + \lambda') \\ & - \frac{1}{2} \sum'_{\mathbf{k}\nu} \frac{\nu J a_{\mathbf{k}}^\nu (1 + d_t(\lambda + \lambda'))}{2\sqrt{(1 + d_t(\lambda + \lambda'))(1 + d_t(\lambda + \lambda') - \nu d_s a_{\mathbf{k}}^\nu)}} \\ & - \sum'_{\mathbf{k}\nu} \frac{\nu J a_{\mathbf{k}}^\nu (1 + \nu d_t a_{\mathbf{k}}^\nu)}{2\sqrt{(1 - \nu d_s a_{\mathbf{k}}^\nu)(1 + \nu d_t a_{\mathbf{k}}^\nu)}}, \end{aligned} \quad (31)$$

and

$$\begin{aligned} \left\langle \frac{\partial H_m}{\partial \bar{t}} \right\rangle = 0 = & \frac{1}{4}J - \mu - 2J\bar{s}^2(\lambda + \lambda') - J(\lambda + \lambda') \\ & + \frac{1}{2} \sum'_{\mathbf{k}\nu} \frac{2J(\lambda + \lambda') (1 + d_t(\lambda + \lambda') - \nu d_s a_{\mathbf{k}}^\nu)}{2\sqrt{(1 + d_t(\lambda + \lambda'))(1 + d_t(\lambda + \lambda') - \nu d_s a_{\mathbf{k}}^\nu)}} \\ & + \sum'_{\mathbf{k}\nu} \frac{\nu J a_{\mathbf{k}}^\nu (1 - \nu d_s a_{\mathbf{k}}^\nu)}{2\sqrt{(1 - \nu d_s a_{\mathbf{k}}^\nu)(1 + \nu d_t a_{\mathbf{k}}^\nu)}}, \end{aligned} \quad (32)$$

in which the first three terms on the right hand side of each expression constitute the classical equations, and the remaining terms the quantum corrections. The notation  $\sum'$  denotes  $\frac{1}{N} \sum$ .

Unconstrained solution of these equations for  $\mu$ ,  $\bar{s}$ , and  $\bar{t}$  at fixed  $\lambda$  and  $\lambda' > \lambda'_c$  gives a set of parameter values which are completely unrelated to those on the disordered side of the QCP, meaning a first-order transition. However, such parameters correspond to modes which are in general all massive, as the spin-wave condition is not obeyed, and have no physical meaning in the present problem of an ordered magnet. This discontinuity between ordered and disordered regimes in an approach combining classical mean-field terms with quantum corrections has been encountered previously in similar circumstances. [7,16,17]

By the Goldstone Theorem, any breaking of a continuous symmetry must be accompanied by the presence of zero-energy excitations, in this case spin waves which are massless in the long-wavelength limit. We proceed by enforcing the third mean-field equation (32) classically: this is precisely the spin-wave condition Eq. (28), and serves both to ensure that the rotation modes are massless at the zone center and to fix the value of one of the three original variables.

The remaining two mean-field equations (30,31) correspond to the pair solved in the disordered phase, now generalized to include finite  $\bar{t}$ . These may be combined to yield a single equation for  $d_t$  as a function of  $\delta\lambda' = \lambda' - \lambda'_c$ , which as  $d_t \rightarrow 0$  returns the critical point equation (29) for  $\lambda'_c$ . Solution of this equation gives a weak first-order transition which may be traced in a linear expansion about  $\lambda'_c$  to the fact that the small  $d_t$  term acts as a cutoff in the  $\mathbf{k}$  summation which provides a logarithmic contribution in three dimensions. The linearized equation has the form

$$d_t(A + B \ln d_t) = C\delta\lambda', \quad (33)$$

which as shown in Fig. 2, describes reentrant behavior of the onset of magnetic order. Numerically, the value  $\bar{t}_0$  (Fig. 2) where the solution at fixed  $\lambda'$  becomes double-valued is 0.048. The  $\lambda'$  axis is however grossly expanded, and the reentrance occurs within the range of values of interladder coupling  $0.118 < \lambda' < 0.121$ . Because the first-order nature of the transition is extremely weak, we may use the formalism developed in this section to describe the features of the ordered magnetic system both qualitatively and on a quantitative basis. Illustration of the zero-temperature solution for the variation of the ordered moment with the interladder coupling is deferred to the following section, where it is presented together with the solutions at finite temperatures.

### III. FINITE-TEMPERATURE SOLUTION AND STATIC SUSCEPTIBILITY

#### Magnon Statistics

To compute the properties of the coupled ladder system at all temperatures, it is necessary first to discuss the statistics of the magnon excitations, which are contained in the thermal occupation function  $n_m(\omega_{\mathbf{k}}^{\pm})$ . [11] The essential feature is that despite the bosonic commutation relations [13] of the single magnon operators, these do not have conventional bosonic statistics because of the constraint (5) on their number, and this has a profound effect on the thermodynamics of the system at intermediate and high temperatures. An approximate approach which gives a good account of the effects of the constrained magnon occupation in the case of the isolated ladder (disordered system) was introduced by Tsunetsugu and coworkers in Ref. [18], and the reader is referred to this work for a detailed discussion. Here we summarize the results of applying this treatment in the ordered magnetic regime.

The following discussion is simplified by the implicit assumption of the presence of an anisotropy field stabilizing one particular spatial direction for the staggered moment, a point to which we shall return in more detail below when considering the susceptibility. This results in a small gap in the spin-wave spectrum, preventing the easy axis from reorienting in an applied field and allowing for a reduction of the energy of one of the modes. In an  $N$ -rung system ( $\frac{1}{4}N$  unit cells) with both rotation ( $\alpha = \sigma \equiv S = \pm 1$ ) and amplitude ( $\alpha = z \equiv S = 0$ ) modes possible at the same wave vector  $\mathbf{k}$ , and in the presence of a magnetic field  $h$ , the free energy per site is given by

$$\tilde{f} = -\frac{1}{2\beta} \ln \{1 + z^z(\beta) + 2 \cosh(\beta h) z^{\sigma}(\beta)\}, \quad (34)$$

where  $z^{\alpha}(\beta) = \sum_{\mathbf{k}}' \exp(-\beta \omega_{\mathbf{k},\alpha})$ , is the partition function for each mode type. The magnon thermal occupation functions per mode in zero field are

$$\tilde{n}_m(\omega_{\mathbf{k}\alpha}) = \frac{1}{e^{-\beta \omega_{\mathbf{k}\alpha}} + 3} \quad (35)$$

in the disordered phase where  $\omega_{\mathbf{k}\alpha} = \omega_{\mathbf{k}z} = \omega_{\mathbf{k}\sigma}$ , and in the ordered phase

$$\tilde{n}_m(\omega_{\mathbf{k}\alpha}) = \frac{e^{-\beta\omega_{\mathbf{k}\alpha}}}{1 + e^{-\beta\omega_{\mathbf{k}z}} + 2e^{-\beta\omega_{\mathbf{k}\sigma}}}. \quad (36)$$

That in the latter two equations the occupation function for a mode  $z$  ( $\sigma$ ) contains a denominator dependent on the energy of a mode  $\sigma$  ( $z$ ) encodes the effects of the constraint. At high temperatures, each of these functions approaches the limiting value of  $\frac{1}{4}$  per mode. The form of the occupation function required in the mean-field equations and denoted in Ref. [11] as  $n_m(\omega_{\mathbf{k}\alpha})$  is that including the zero-point term, *i.e.* the analog of the bosonic  $\frac{1}{2} \coth\left(\frac{1}{2}\beta\omega_{\mathbf{k}\alpha}\right)$ , and is given by  $n_m(\omega_{\mathbf{k}\alpha}) = \frac{1}{2} + \tilde{n}_m(\omega_{\mathbf{k}\alpha})$ .

### Mean-Field Solutions

Considering first the approach to the transition from the disordered side, in Fig. 3 is shown the evolution of the spin gap  $\Delta$ , the minimum of the triply degenerate massive magnon dispersion, with interladder coupling at temperatures between 0 and  $0.5J$ . The zero-temperature graph is that shown already in Ref. [11]. Solution of the mean-field equations at finite temperatures is marginally more complicated because the initial system of two variables may not be reduced to a single one in the same manner. As the temperature is increased, the disordered phase becomes more robust as might be expected, and a larger interladder coupling is required to stabilize magnetic order. The spin gap in the isolated ladder is found also to increase with temperature, although this rise is somewhat more linear above  $T = 0.1J$  than would be given by the simplest possible formulation,  $\Delta = \sqrt{\Delta_0^2 + T^2}$ .

In the ordered phase, the characteristic parameter varying with the coupling constant is  $\bar{t}$ , which gives the extent of staggered moment formation. This is shown in Fig. 4 for the same temperatures. The ordered moment rises abruptly at the transition, with no obvious indication at any temperature of the reentrant behavior discussed in the previous section, and then less steeply thereafter. However, the logarithmic evolution of the ordered moment given in Eq. (33) is manifest in a  $\ln$ - $\ln$  plot, and precludes the extraction of a

power-law mean-field exponent from data within a range  $\Delta\lambda' \simeq 0.15$  of the transition. At high values of the interladder coupling, the ordered moment falls short of the limiting value  $\bar{t} = \frac{1}{\sqrt{2}}$  as  $\lambda' \rightarrow 1$ , showing that in the bond-operator description of the isotropic limit there remains some admixture of rung singlets with the ordered spins, a consequence of quantum fluctuations.

Turning now to the physical situation of a fixed interladder coupling constant at variable temperature, it is clear from Fig. 3 that any system will be disordered at high temperature. By solution of a pair of equations analogous to the zero-temperature critical-point equation (29), this phase boundary is found in the plane of  $T$  and  $\lambda'$ , giving the Néel temperature shown in Fig. 5. Because  $T_N$  in this figure is measured in units of  $J \sim 1400K$ , it is evident that the real material  $\text{LaCuO}_{2.5}$ , with a Néel temperature [9] of 117K, is located extremely close to the QCP (in fact at  $\lambda' = 0.127$ ). We will use for illustration the interladder coupling value  $\lambda' = 0.13$ , for which the dispersion relations have already been sketched in Fig. 1(c). The dispersion curves in the physical Brillouin zone are now shown quantitatively in Fig. 6 for this parameter choice, at which the ordered moment has the value  $\bar{t} = 0.14$  and  $T_N = 0.105J$ .

### Static Susceptibility

The physical quantity most readily measurable which gives direct information about the magnetic state of a spin system is the static susceptibility  $\chi(T)$ , and for this reason it has been the subject of extensive discussions [1,18] and measurements in a variety of ladder systems. [8,19] The susceptibility per site is

$$\chi(T) = - \left. \frac{\partial^2 \tilde{f}}{\partial h^2} \right|_{h=0}, \quad (37)$$

which from Eq. (34) yields in the disordered phase [18]

$$\chi(T) = \beta \frac{z^\alpha(\beta)}{1 + 3z^\alpha(\beta)}. \quad (38)$$

This is illustrated over a wide temperature range in Fig. 7(a), where it is clear that the interladder coupling has an effect only at low  $T$ , while the remainder of the graph is well described by the numerical results for the isolated ladder. [18] The situation at low temperatures is displayed in the inset, which shows that as the critical coupling is approached  $\chi(T)$  rises more rapidly with temperature. The nature of this increase may be studied by examining the function

$$g(T) = T^2 \frac{\chi'(T)}{\chi(T)}, \quad (39)$$

in which  $\chi'$  denotes the temperature derivative. For the a system with spin gap [18]  $\Delta$ ,  $\chi(T) = T^{-\alpha} e^{-\beta\Delta}$  and  $g = \Delta - \alpha T$ , while for a power-law dependence  $\chi(T) = aT^\alpha$ , as might be expected in a critical regime,  $g = \alpha T$ . Fig. 7(b) shows this function at low- $T$  for several values of the coupling constant  $\lambda'$ , demonstrating clearly the evolution of the system with interladder coupling from a spin liquid with the spin gap  $\Delta_0 \simeq 0.5J$  and power  $\alpha = \frac{1}{2}$  prefactor of the isolated ladder, to a quantum critical phase in three dimensions, where  $\alpha = 2$ . These results have a straightforward interpretation from the thermal excitations of a dilute gas of (noninteracting) triplet magnons whose dispersion is quadratic about a spin gap  $\Delta$ , and becomes linear as  $\Delta \rightarrow 0$ . At the QCP the susceptibility is due to excitations of spin waves, with temperature dependence determined only by system dimensionality.

The calculation of the susceptibility in the ordered phase may proceed in one of two ways: for an ideal system with no interaction between the spins and the real-space or lattice coordinates, the ordered moment simply reorients in an applied field to be perpendicular, *i.e.* a spin-flop transition. For a system with an easy-axis anisotropy, the spin waves acquire a mass proportional to the effective anisotropy field  $h_a$ , and this allows the moment direction to remain stable under application of a parallel field. For a review of both situations see Ref. [20]. The susceptibility is computed in the zero-field limit, which may always be taken as an external field smaller than the intrinsic anisotropy energy, so we restrict our attention to the simplest case of the susceptibility contribution from normal mode excitations for the case of pinned moment direction in a parallel field.

In addition to the part due to excitation of normal modes, the susceptibility in the ordered phase contains a constant part due to the presence of the finite moment, and so may be represented as

$$\chi(T) = \chi_0(T) + \chi_{\text{exc}}(T). \quad (40)$$

$\chi_{\text{exc}}(T)$  is computed by analogy with the disordered phase from the free energy of the modes which may be excited, and is given by

$$\chi_{\text{exc}}^{\parallel}(T) = \beta \frac{z^{\sigma}(\beta)}{1 + z^z(\beta) + 2z^{\sigma}(\beta)}. \quad (41)$$

Because this part has its leading contributions from the spin-wave modes with dispersion  $\omega_{\mathbf{k}\sigma}$ , it can be expected always to have a quadratic  $T$  dependence at low temperatures. The component due to application of a perpendicular field is similar, but slightly more involved because the evolution of the mode  $\omega_{\mathbf{k}z}$  with field is not linear for a finite gap, a point which will be illustrated below. The numerator contains also a term in  $z^z(\beta)$ , which is much smaller than the spin-wave contribution when the mass of the  $z$  mode is finite, and higher-order terms which cancel at the transition. The dominant feature of the temperature dependence remains the  $T^2$  part due to the spin-wave contribution, with a smaller prefactor. On averaging over the crystallite directions in a polycrystalline sample,  $\chi_{\text{exc}}(T) = \frac{1}{3}\chi_{\text{exc}}^{\parallel}(T) + \frac{2}{3}\chi_{\text{exc}}^{\perp}(T)$ .

Similarly, the static part in the anisotropy-pinned case may be written as  $\chi_0(T) = \frac{2}{3}\chi_0^{\perp}$  for a polycrystalline sample, as only the transverse part has a finite value and this will be observed as an average over all crystallite orientations.  $\chi_{0\perp}$  may be computed in the bond-operator formalism by considering the additional term in the mean-field Hamiltonian in the presence of a finite magnetic field  $\mathbf{h}$ ,

$$\sum_i \mathbf{h} \cdot (\mathbf{S}_{l_i}^1 + \mathbf{S}_{r_i}^1 + \mathbf{S}_{l_i}^2 + \mathbf{S}_{r_i}^2) = -i\epsilon_{\alpha\beta\gamma} \sum_i (t_{i\beta}^{1\dagger} t_{i\gamma}^1 + t_{i\beta}^{2\dagger} t_{i\gamma}^2). \quad (42)$$

The evolution of the bond-operator modes of a ladder system with application of a magnetic field will be presented elsewhere. Here we state the result that in general a field component  $h_{\alpha}$  acts to create an ordered moment  $t_m$  in the operators  $t_{\beta}$  and  $t_{\gamma}$ , where  $\alpha \neq \beta \neq \gamma$ . In



the presence of a finite, staggered  $\langle t_z \rangle = \bar{t}$ , application of a small field  $h_x$  stabilizes a finite, staggered ordered moment  $\langle -it_y \rangle \equiv \bar{t}_m$ . One of the spin-wave modes is unaffected by the field and the induced moment and one increases linearly with  $h$ , while the amplitude mode energy rises only quadratically with  $h$ . We find that  $\bar{t}_m \propto \bar{t}h$ , and that the magnetization per site stabilized by a small field  $h_x$  is  $\bar{m}_x = -\frac{1}{2}\bar{t}_m\bar{t}$ , giving for the transverse part  $\chi_0^\perp = \frac{\partial \bar{m}_x}{\partial h_x} \propto \bar{t}^2$ . As a function of interladder coupling, this contribution appears very similar to the results in Fig. 5 for  $\bar{t}$ .  $\chi_0^\perp$  vanishes approximately in the manner of a second-order transition as the temperature is increased towards  $T_N$ . When the same formalism is applied to the case of a longitudinal field, the ordered moment is  $O(\bar{t}_m^2)$  and it is clear that  $\chi_0^\parallel$  is vanishing, so that the total  $\chi^\parallel$  has  $T^2$  contributions only.

In Fig. 8 is shown the full static susceptibility  $\chi(T)$  (40) for a variety of values of interladder coupling in the ordered phase,  $\lambda' > \lambda'_c$ . The curves begin at the finite value of  $\chi_0(T=0)$  calculated in the preceding paragraphs, and their variation with temperature is approximately quadratic because  $\chi_0(T)$  is nearly constant at low  $T$ , particularly for values of the interladder coupling not in close proximity to the critical point. Because the scale of  $\chi_0$  is significantly smaller than that of  $\chi_{\text{exc}}$ , the second-order transition in  $\chi_0(T)$  at  $T_N$  appears as a minor downward cusp. The results compare very well with highly accurate Quantum Monte Carlo studies on very large systems by Troyer *et al.* [12], which show the transition from spin liquid to ordered magnet occurring very close to  $\lambda' = 0.12$ , and continuous evolution of the susceptibility from an exponential form in the disordered phase to a quadratic variation at the critical point with an additive constant part which grows continuously on moving to the ordered side. Quantitatively, the magnitude of the peak susceptibility is some 15% greater in the mean-field theory, and that of the constant parts approximately 20% smaller at common values of the coupling in the ordered phase. One may fit the measured static susceptibility [8] to the form  $\chi(T) = a + bT^2$  at low temperatures, and quadratic temperature dependence is found [12] to give a good account of the data. The intrinsic susceptibility  $\chi_0$  of the coupled ladder system is very difficult to extract from the constant  $a$ , as this requires detailed knowledge of core atomic susceptibility terms, and we note only the qualitative

result that all terms involved are very small, a further indication of the proximity of the system to the QCP. That the mean-field theory is in such generally good agreement with the numerical results, which for an unfrustrated spin system and with demonstrably negligible finite-size corrections can be taken to be essentially exact, is presumed to be primarily a consequence of the three-dimensionality of the ordered magnetic system.

#### IV. DYNAMIC MAGNETIC PROPERTIES

In the preceding section we have deduced that the  $\text{LaCuO}_{2.5}$  system is magnetically ordered but located close to the QCP, as a result of which the transition temperature and ordered moment are small. One consequence is that the magnetic modes corresponding to fluctuations in the amplitude of the ordered moment, which in a conventional magnet are high-lying and play no role in determining the low-energy properties of the system, should have only a small mass here. In this section we study the dynamic magnetic properties of such a system to isolate those features due to the presence of the amplitude mode and predict the ways in which these may be identified definitively by experiment.

We focus directly on the dynamic structure factor measured by neutron scattering, which may be written following Ref. [21] in the form

$$S^R(\mathbf{q}, \omega) = \frac{1}{2\pi} \sum_{\alpha\beta} (\delta_{\alpha\beta} - \hat{q}_\alpha \hat{q}_\beta) \sum_{i, \langle ij \rangle, \tau, \tau'} \frac{1}{4} g_\tau g_{\tau'} F_\tau^*(\mathbf{q}) F_{\tau'}(\mathbf{q}) \\ \times \int_{-\infty}^{\infty} dt e^{-i\omega t} \langle \exp(-i\mathbf{q} \cdot \mathbf{r}_{i,\tau}(0)) \exp(i\mathbf{q} \cdot \mathbf{r}_{i+\mathbf{r}_{ij},\tau'}(t)) \rangle \langle S_{i+\tau}^\alpha(0) S_{i+\mathbf{r}_{ij}+\tau'}^\beta(t) \rangle, \quad (43)$$

Here  $i$  and  $j$  denote unit cells, and  $\tau$  and  $\tau'$  are vectors specifying the locations of the atoms in each cell.  $F_\tau(\mathbf{q})$  is the magnetic form factor which describes the spatial extent of the spin density around the site  $\tau$ , and  $g_\tau$  is the Landé factor. In this expression the space and spin variables are partially factorized, and each expectation value can be separated into a constant part, corresponding to elastic scattering, and a time-dependent part responsible for inelastic processes.

We consider first the elastic magnetic component, in order to isolate those Bragg peaks

with the highest intensity about which one may measure the dynamical structure factor most readily, and also to discuss the nature of the magnetically ordered state. In Ref. [11] it was assumed that the interladder coupling in  $\text{LaCuO}_{2.5}$  was AF. This assumption was made on the basis that ferromagnetic coupling, which relies on Hund's Rule coupling between orbitals on an atom in the superexchange path, is generally weaker than AF coupling energy scales, and that because the system is one of low symmetry it was likely that the latter would have appreciable components on certain paths. In fact this assumption was not tested in detail, and the tight-binding fit to the Local Density Approximation (LDA) bandstructure was made using a single Wannier orbital on each Cu site, which was taken to be a mixture (due to the low symmetry) of Cu  $3d_{x^2-y^2}$ - and  $3d_{3z^2-r^2}$ -centred orbitals in the pyramidal  $\text{CuO}_5$  system. The good agreement obtained with this procedure appeared to justify the assumptions made, but did not rule out alternative parameter combinations. The results of the preceding section of this work provide a more reliable means of estimating the magnitude of the interladder coupling. Recently a quantitative effort has been made by Mizokawa *et al.* [22] to understand the superexchange parameters in  $\text{LaCuO}_{2.5}$ . These authors deduce some of the parameters of the electronic structure from measurements made by Cu  $2p$  core-level spectroscopy, and use these in Hartree-Fock calculations. They conclude that the magnetically ordered state of lowest energy is that where the AF coupled spins in each ladder are ferromagnetically coupled between the ladders, and that the magnitude of the interladder interaction is less than  $0.1J$ . Superexchange estimates involving competing exchange paths are difficult, and can involve significant errors due to computing small differences between large numbers. Nevertheless this is the most systematic study performed on the system to date. We note that the results of the preceding sections are essentially independent of the sign of the coupling ratio  $\lambda'$ , which acts only to exchange the branch indices  $\nu = \pm$ .

The elastic magnetic scattering is described by the static structure factor, the time-independent part of Eq. (43), and has finite components

$$S_s^R(\mathbf{G}) = N \langle S^z \rangle^2 \left( 1 - (\mathbf{G} \cdot \hat{\mathbf{z}})_{av}^2 \right) \left[ \frac{1}{2} g F(\mathbf{q}) \right]^2 \mathcal{F}(\mathbf{G}) \quad (44)$$

only at the reciprocal lattice vectors  $\mathbf{G}$ , which are the magnetic Bragg peaks. Here  $\hat{z}$  is the direction of the ordered spin moment in real space, and is not yet known. In cuprates, the coupling of the spin system to the lattice which determines this direction is generally very weak, although by comparison with the parent phases of tetragonal high-temperature superconducting materials the spins may be expected to align along either the rungs or chains of the ladders.  $\langle S^z \rangle$  is the magnitude of the ordered moment, and for the coupling value  $\lambda' = 0.13$  is of magnitude  $\sqrt{2t} \simeq 0.2$ . Thus the square of this quantity yields only a 4% effect, rendering the elastic scattering rather weak close to the QCP.

$$\mathcal{F}(\mathbf{G}) = \sum_{\tau, \tau'} (-1)^{(\tau + \tau')} e^{i\mathbf{G} \cdot (\tau - \tau')} \quad (45)$$

is the structure function, obtained by summing over the sites in the unit cell, in which the convention used with the site labels  $\tau$  is such as to ensure that each  $\uparrow$  and  $\downarrow$  spins introduce factors of the opposite sign, corresponding to the spin density distribution around each site. The appropriate site labeling for one plane of Cu atoms is shown in Fig. 9(a) for the simple AF structure function, which we denote as Type I AF, and in Fig. 9(b) for the case with ferromagnetic coupling between the AF ladders, which we denote as Type II AF. It is straightforward to calculate  $\mathcal{F}(\mathbf{G})$ , and the results are expressed by quoting the reciprocal lattice vector  $\mathbf{G}$  of the magnetic Brillouin zone as  $(h, k, l)$ , with  $o$  and  $e$  denoting odd and even integers respectively. For the Type I configuration

$$\mathcal{F}(\mathbf{G}) = \begin{cases} 64 \cos^2 G_x a_x \sin^2 G_y a_y & (e, e, o), (o, o, o) \\ 64 \sin^2 G_x a_x \cos^2 G_y a_y & (e, o, o), (o, e, o) \\ 0 & l \text{ even} \end{cases} \quad (46)$$

while for Type II the results are identical with  $[x \leftrightarrow y]$ ; the displacement vector components  $a_x$  and  $a_y$  are shown in Fig. 9. These quantities, normalized to unity, are shown in Fig. 10 for the two configurations in any reciprocal-space plane of odd  $l$  and for values of  $h$  and  $k$  between 0 and 10. It is evident that there are Bragg peaks of nearly maximal amplitude, and so the best points in the reciprocal zone around which to investigate the dispersion of the dynamical modes would be for example  $(2, 0, o)$  and  $(0, 1, o)$  in Type I, or  $(3, 0, o)$ ,

$(0, 4, o)$  and  $(5, 1, o)$  in Type II. Because the two configurations differ significantly in the locations of strong Bragg peaks, it should be possible by diffractometry to determine the sign of the interladder superexchange.

Turning to the dynamical structure factor as it might be observed (in a single-crystal sample) around one Bragg peak, the factor of interest is the spin part  $\int dt e^{i\omega t} \langle S_{\mathbf{q}}^{\alpha}(0) S_{-\mathbf{q}}^{\beta}(t) \rangle$ , from which the spatial dependence on the crystal structure has been removed. In order to compute this quantity in terms of the bond-operator eigenmodes, we take first the rung combinations [14]

$$S_{\mathbf{q}\alpha}^{\pm}(t) = \sum_i e^{i\mathbf{q} \cdot \mathbf{r}_i} [S_{l_i\alpha}(t) \pm S_{r_i\alpha}(t)], \quad (47)$$

and then combine the variables on the two rungs in the reduced, AF ordered unit cell to give

$$\begin{aligned} S_{\mathbf{q}\alpha}^{+\pm} &= -i\epsilon_{\alpha\beta\gamma} \sum_{\mathbf{k}} \left( t_{\mathbf{k}+\mathbf{q}\beta}^{1\dagger} t_{\mathbf{k}\gamma}^1 \mp t_{\mathbf{k}+\mathbf{q}\beta}^{2\dagger} t_{\mathbf{k}\gamma}^2 \right) \\ S_{\mathbf{q}\alpha}^{-\pm} &= \bar{s} \left( t_{\mathbf{q}\alpha}^1 + t_{-\mathbf{q}\alpha}^{1\dagger} \right) \pm \bar{s} \left( t_{\mathbf{q}\alpha}^2 + t_{-\mathbf{q}\alpha}^{2\dagger} \right). \end{aligned} \quad (48)$$

The final expression for the structure factor

$$S^R(\mathbf{q}, \omega) = \sum_{\alpha} \sum_{\mu\nu\eta\rho=\pm} \int_{-\infty}^{\infty} dt e^{i\omega t} \langle S_{\mathbf{q}\alpha}^{\mu\nu}(0) S_{-\mathbf{q}\alpha}^{\eta\rho}(t) \rangle \quad (49)$$

is a sum over the three spin indices (for unpolarized neutron scattering) and all sign combinations of  $S^{\pm\pm}$ , and its evaluation is aided by extensive cancellation of terms. For scattering studies at low temperatures, where very few excited states are occupied and these only singly, we may from their bosonic commutation relations [13] compute the thermal expectation value by summation over bosonic Matsubara frequencies. The two types of component which emerge from Eq. (49) are

$$S^{R-}(\mathbf{q}, \omega) = \sum_{\alpha} \pi \left( \bar{s}^2 + \bar{t}^2 \right) \left( \cosh 2\theta_{\mathbf{q}}^{\alpha} - \sinh 2\theta_{\mathbf{q}}^{\alpha} \right) \left[ n_{\mathbf{q}}^{\alpha} + \Theta(\omega) \right] \delta \left( \omega_{\mathbf{q}}^{\alpha} - |\omega| \right) \quad (50)$$

$$\begin{aligned} S^{R+}(\mathbf{q}, \omega) &= \sum_{\mathbf{k}\alpha\neq\beta} \left\{ \left( \cosh 2(\theta_{\mathbf{k}+\mathbf{q}}^{\alpha} - \theta_{\mathbf{k}}^{\beta}) + 1 \right) n_{\mathbf{k}}^{\beta} (n_{\mathbf{k}}^{\alpha} + 1) \delta \left( \omega_{\mathbf{k}+\mathbf{q}}^{\alpha} - \omega_{\mathbf{k}}^{\beta} - \omega \right) \right. \\ &\quad \left. + \frac{1}{2} \left( \cosh 2(\theta_{\mathbf{k}+\mathbf{q}}^{\alpha} - \theta_{\mathbf{k}}^{\beta}) - 1 \right) \left[ n_{\mathbf{k}}^{\alpha} + \Theta(\omega) \right] \left[ n_{\mathbf{k}}^{\beta} + \Theta(\omega) \right] \delta \left( \omega_{\mathbf{k}+\mathbf{q}}^{\alpha} + \omega_{\mathbf{k}}^{\beta} - |\omega| \right) \right\}, \end{aligned} \quad (51)$$

in which the hyperbolic trigonometric functions are the coefficients of the Bogoliubov transformation, [11] and the  $n_{\mathbf{k}}$  are thermal occupation functions. Errors due to the constraint on magnon occupations are negligible at low temperatures, and may in fact be taken into account fully by a more general formulation of the scattering expression, which gives different thermal occupation functions  $n_{\mathbf{k}}$ .  $S^{R-}(\mathbf{q}, \omega)$  (50) appears with coefficient  $(\bar{s}^2 + \bar{t}^2)$  for contributions from the  $\sigma$  components of the spins, due to the presence of the ordered moment in  $t_z$ , and with coefficient  $\bar{s}^2$  otherwise. It has the simple interpretation of scattering processes involving magnon creation or destruction, and will be seen as a broadened  $\delta$ -function line along  $(\mathbf{q}, \omega_{\mathbf{q}\alpha})$  corresponding to the magnon dispersion relations.  $S^{R+}(\mathbf{q}, \omega)$  (51) describes magnon-magnon scattering (first line) and pair creation or destruction processes (second line), each involving magnons of a different type, and so will have  $(\sigma, \sigma)$  and  $(\sigma, z)$  components which could in principle be distinguished by polarized neutron scattering.

The dynamic structure factor  $S^{R-}(\mathbf{q}, \omega)$  for magnon creation ( $\omega > 0$ ) is shown in Fig. 11, and as stated above is found to consist of a series of peaks at the dispersion relations of all magnon branches. A small broadening is inserted by hand in the calculation. In the disordered system (Fig. 11(a)) there are four triply degenerate branches in the physical unit cell, and the lowest of these has a gap at the bottom of its band ( $q = 0$ ), as required for a spin liquid. In the ordered system (Fig. 11(b)), this gap has vanished, and branches are split into their  $\sigma$  and  $z$  components. In the lowest-lying branch, the intensity of the spin-wave peak diverges as  $q \rightarrow 0$  and the magnetic Bragg peak is approached, while the corresponding  $z$  mode appears at the energy  $\omega = 0.29J$  at the chosen value of interladder coupling. This energy splitting is expected to be resolvable, and so the amplitude mode should be detected as a neighboring peak, or at least as a significant shoulder to the elastic peak, and to each of the dispersion branches. The component  $S^{R+}(\mathbf{q}, \omega)$  for two-magnon scattering and pair creation has an intensity between one and two orders of magnitude lower than that from magnon creation, and so will be barely detectable. Because inelastic neutron scattering couples directly to the one-magnon process, it is the best technique to observe a clear signature of the low-lying amplitude mode.

We have considered also the expected form of the intensity  $I(\omega)$  in a Raman light scattering experiment on the magnetically ordered but nearly critical system. Unambiguous spectroscopic evidence for the amplitude mode, as in the magnon creation signal expected in the neutron scattering cross section, would be provided by one-magnon processes with a significant weight. Following Fleury and Loudon, [23] it is clear that in this system neither the magnetic-dipole nor electric-dipole first-order interactions detailed by these authors can provide appreciable signals. Concluding for completeness with second-order light scattering, we have computed the  $\langle(\mathbf{S}_i \cdot \mathbf{S}_j)(\mathbf{S}_i \cdot \mathbf{S}_j)\rangle$  correlation function which gives the intensity in a spin-only model. [24] We find a “ $3J$ ” peak due to scattering of zone-boundary magnons in the ladder ( $\pm k_z$ ) direction, and that this peak is broadened in the presence of an amplitude mode split off from the spin wave band in an AF system close to the QCP. However, mindful of the facts that measured spectra are not fully explained by two-magnon scattering considerations, and that these are found to be anomalously broad in other cuprate materials, we conclude that Raman scattering is unlikely to be a suitable probe of the dynamics of the amplitude mode.

## V. CONCLUSION

We have presented a theoretical description of the three-dimensionally coupled spin ladder system which is realized in the insulating compound  $\text{LaCuO}_{2.5}$ . This spin configuration is such that for weak interladder magnetic coupling the ground state is the spin-liquid phase characteristic of the isolated ladder, while for larger coupling values an unfrustrated, magnetically ordered state is expected. We employ a representation based on singlet and triplet bond operators on each rung of the ladders to obtain a uniform description of both phases within the same framework.

Within the mean-field approach to the bond-operator formalism, solution at zero temperature gives the interladder coupling at the QCP as  $J' = 0.121J$ . The transition is found to be very weakly first order, and the increase of the ordered moment to be logarithmic in

the coupling ratio  $\lambda' - \lambda'_c$  in the vicinity of the transition, with the mean-field exponent recovered at higher  $\lambda'$ . Finite-temperature solutions are obtained by incorporating the constraint on the triplet excited states into an effective magnon statistics, and show the increase with temperature of the disordered regime and the critical coupling, allowing the deduction of the Néel temperature.

The real material has an ordering temperature extremely small on the scale of the superexchange parameter  $J$  within the ladders, implying that it is located very close to the QCP on the ordered side. In this case the magnon mode corresponding to amplitude fluctuations of the ordered moment has only a small gap at the bottom of its band, and will contribute to the low-energy dynamic and thermodynamic properties of the system. The constant part of the static susceptibility is proportional to the square of the ordered moment and is small, reconciling measured susceptibility data with the fact that the system is ordered. The part of the static susceptibility due to thermal excitation of modes of the system increases quadratically with temperature for spin waves in three dimensions. The results of the mean-field theory are supported by comparison with the detailed Quantum Monte Carlo studies of Troyer *et al.* [12]. We have demonstrated that the low-lying amplitude mode, which is unique to this type of AF, contributes to the dynamical response function. Inelastic neutron scattering is an especially suitable probe for investigating this mode as it may access one-magnon excitation processes, and we have presented an explicit calculation of its effects for comparison with experiment.

In closing, for a system so close to the QCP we may speculate on ways of controlling the tuning parameter represented by the interladder coupling in order to pass through the transition. As discussed in the preceding section, the superexchange processes contributing to the interladder magnetic interaction are not well understood, but the coupling is known to be a decreasing function of the bond angle away from  $180^\circ$ . It may be possible by application of hydrostatic pressure, or better uniaxial pressure along the  $x$ - or  $y$ -axis of a single crystal, to cause an alteration of this bond angle significant enough to measure, at



least as a raising or lowering of  $T_N$  as deduced from  $\frac{1}{T_1}$  by NMR. As an alternative to physical pressure it is possible [25] also to apply chemical pressure by substituting other trivalent atoms for La. In  $\text{LaCuO}_{2.5}$  the bond angle is found to increase on substitution of Y for La, while it is decreased in equal amount by substitution of Nd. We await with interest more detailed results on the evolution of the magnetic state, which may provide evidence of the system being moved through the QCP. However, for a random distribution of substituents there will be a random distribution of local distortions, from which one may deduce only an average value for the bond angle and interladder coupling, so that interpretation within the above framework will be less transparent. Finally, as we have shown in the preceding sections, the changes in many bulk quantities across the quantum critical regime remain essentially smooth, and it will be necessary to adopt a criterion based on the appearance of the staggered moment or the associated massive mode for unambiguous identification of the transition point.

## ACKNOWLEDGEMENTS

We are grateful to Z. Hiroi, T.-K. Ng, S. Sachdev, M. Sigrist, M. Troyer and M. E. Zhitomirsky for helpful discussions.

## REFERENCES

- [1] E. Dagotto and T. M. Rice, *Science* **271**, 618 (1996), and references therein.
- [2] Z. Hiroi, M. Azuma, M. Takano and Y. Bando, *J. Solid State Chem.* **95**, 230 (1991).
- [3] T. M. Rice, S. Gopalan and M. Sigrist, *Europhys. Lett.* **23**, 445 (1993).
- [4] M. Uehara, T. Nagata, J. Akimitsu, H. Takahashi, N. Mori, and K. Kinoshita, *J. Phys. Soc. Jpn.* **65**, 2674 (1996).
- [5] S. Chakravarty, B. I. Halperin, and D. R. Nelson, *Phys. Rev. B* **39**, 2344 (1989).
- [6] A. V. Chubukov, S. Sachdev, and J. Ye, *Phys. Rev. B* **49**, 11919 (1994).
- [7] see S. Sachdev, e-print cond-mat/9606083, and references therein.
- [8] Z. Hiroi and M. Takano, *Nature* **377**, 41 (1995).
- [9] S. Matsumoto, Y. Kitaoka, K. Ishida, K. Asayama, Z. Hiroi, N. Kobayashi, and M. Takano, *Phys. Rev. B* **53** 11942 (1996).
- [10] R. Kadono, H. Okajima, A. Yamashita, T. Yokoo, J. Akimitsu, N. Kobayashi, Z. Hiroi, M. Takano, and K. Nagamine, *Phys. Rev. B* **54** 9628 (1996).
- [11] B. Normand and T. M. Rice, *Phys. Rev. B* **54**, 7180 (1996).
- [12] M. Troyer, M. E. Zhitomirsky, and K. Ueda, *Phys. Rev. B* (in press).
- [13] S. Sachdev and R. Bhatt, *Phys. Rev. B* **41**, 9323 (1990).
- [14] S. Gopalan, T. M. Rice, and M. Sigrist, *Phys. Rev. B* **49**, 8901 (1994).
- [15] C. Kittel, *Quantum Theory of Solids*, (John Wiley & Sons, New York, 1987).
- [16] S. Sachdev, *Ann. Phys.* **251**, 76 (1996).
- [17] T.-K. Ng, private communication.
- [18] M. Troyer, H. Tsunetsugu, and D. Würtz, *Phys. Rev. B* **50**, 13515 (1994).

- [19] M. Azuma, Z. Hiroi, M. Takano, K. Ishida, and Y. Kitaoka, Phys. Rev. Lett. **73**, 3463 (1994).
- [20] F. Keffer in Handbuch der Physik XVIII/2, Ferromagnetism, (Springer, Berlin, 1966).
- [21] G. L. Squires, Introduction to the Theory of Thermal Neutron Scattering, (Cambridge University Press, Cambridge, 1978).
- [22] T. Mizokawa, private communication.
- [23] P. A. Fleury and R. Loudon, Phys. Rev. **166**, 514 (1968).
- [24] B. S. Shastry and B. I. Shraiman, Phys. Rev. Lett. **65**, 1068 (1990).
- [25] Z. Hiroi, private communication.

## FIGURES

FIG. 1. Schematic representation of triplet excitation mode structure  $\omega_{\mathbf{k}\alpha}$  in  $\text{LaCuO}_{2.5}$  system. (a) Disordered (spin liquid) phase at low interladder coupling  $\lambda' < \lambda'_c$ : triply-degenerate, massive modes. (b) Quantum Critical Point  $\lambda' = \lambda'_c$ : triply-degenerate spin waves. (c) Magnetically Ordered phase at larger interladder couplings  $\lambda' > \lambda'_c$ , with halved Brillouin zone.

FIG. 2. Graphical representation of weak first-order part in transition of  $\bar{t}(\lambda')$ , from solution of Eq. (33).

FIG. 3. Spin gap as a function of interladder coupling at several values of temperature, illustrating monotonic decrease of  $\Delta$  with increasing  $\lambda'$  towards a vanishing at the point of transition from disordered to magnetically ordered phase.

FIG. 4. Magnitude of ordered moment  $\bar{t}$  as a function of interladder coupling at several values of temperature, illustrating abrupt increase from the weak first-order transition at  $\lambda'_c$ , followed by more gradual progress towards nearly-full polarization.

FIG. 5. Néel Temperature  $T_N$  as a function of interladder coupling. For  $\text{LaCuO}_{2.5}$ , the measured value  $T_N = 117\text{K} < 0.1J$  [9] indicates very close proximity to the QCP.

FIG. 6. (a) Static susceptibility  $\chi(T)$  for several values of interladder coupling in the disordered phase. Deviations from the behavior of the isolated ladder are observed only at temperatures  $T < \lambda'J$  below the scale of the coupling energy. This regime is expanded in the inset. (b) The function  $f(T)$  (39) for four values of  $\lambda'$  spanning the disordered phase, illustrating the change from exponentially activated to quadratic susceptibility with decreasing spin gap.

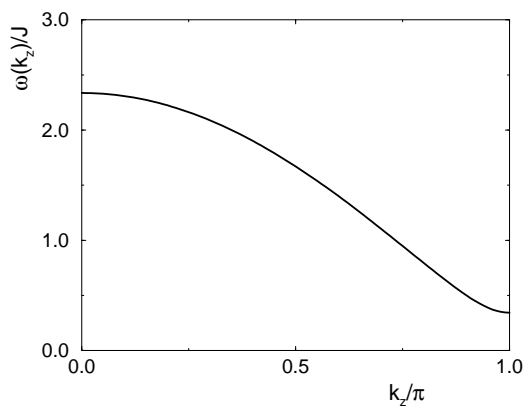
FIG. 7. Magnon dispersion relations in physical Brillouin zone along the lines  $\text{X}\Gamma$  and  $\Gamma\text{Z}$  for magnetically ordered system  $\lambda' = 0.13$ . All branches  $\sigma$  are doubly degenerate, and the lower  $\omega_{\mathbf{k}}^{z+}$  line is the amplitude mode with a small mass ( $0.29J$  here) near the QCP.

FIG. 8. Static susceptibility  $\chi(T)$  for several values of interladder coupling in the ordered phase. The constant part  $\chi_0$  rises, at first rapidly, with  $\lambda'$  away from  $\lambda'_c$ . Small downward cusps appear at  $T = T_N$ , marking the second-order vanishing of  $\chi_0$ . Isolated-ladder character is recovered at high temperature.

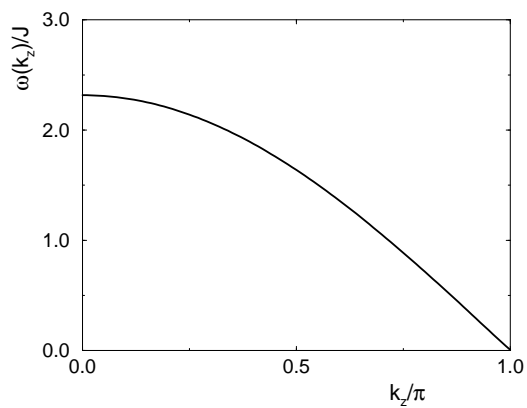
FIG. 9. Unit cell structure and labeling for one plane of atoms in magnetically ordered material, for computation of structure function  $\mathcal{F}(\mathbf{G})$  (45). Intraladder coupling (perpendicular to plane of diagram) is always AF, whence unit-cell doubling. (a) Type I AF configuration. (b) Type II AF configuration.

FIG. 10. Structure function  $\mathcal{F}(\mathbf{G})$  at reciprocal lattice points  $(h, k, l=\text{odd})$ , for  $0 \leq h, k \leq 10$ . (a) Type I AF. (b) Type II AF. The full static structure factor requires also multiplication by the square of the ordered moment, and so will be rather small for a system close to the QCP.

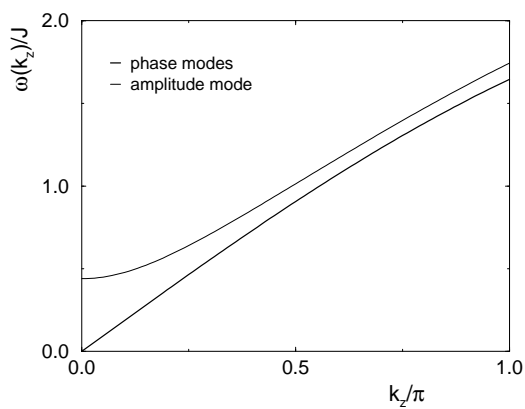
FIG. 11. Dynamic structure factor  $S^R(q_z, \omega)$  expected from inelastic neutron scattering, illustrating contributions from magnon creation processes, which appear as a broadened  $\delta$ -function at the dispersion branches  $\omega_\alpha(q_z)$  (a) Disordered system,  $\lambda' = 0.05$ : all four branches in physical Brillouin zone are triply degenerate, and there is a gap in excitation energy  $\omega$  to the first mode at  $q = 0$ . (b) Ordered system close to the critical point,  $\lambda' = 0.13$ : branches are split into  $\sigma$  and (massive)  $z$  modes. For the lowest branch, the spin-wave scattering amplitude diverges as  $q^2$  as  $q \rightarrow 0$ , forming the elastic peak. The signature of the massive but low-lying amplitude mode is the peak dispersing from  $\omega = 0.29J$  at  $q = 0$ .



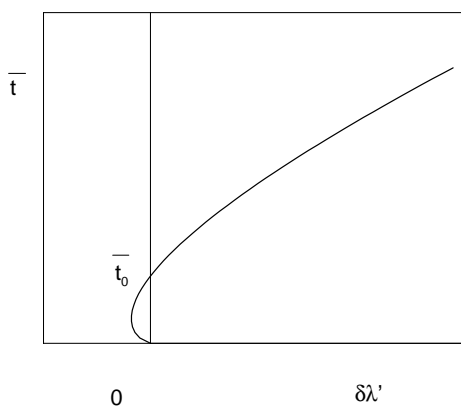
1(a)



1(b)



1(c)



2

Figs. 1 & 2, B. Normand and T. M. Rice

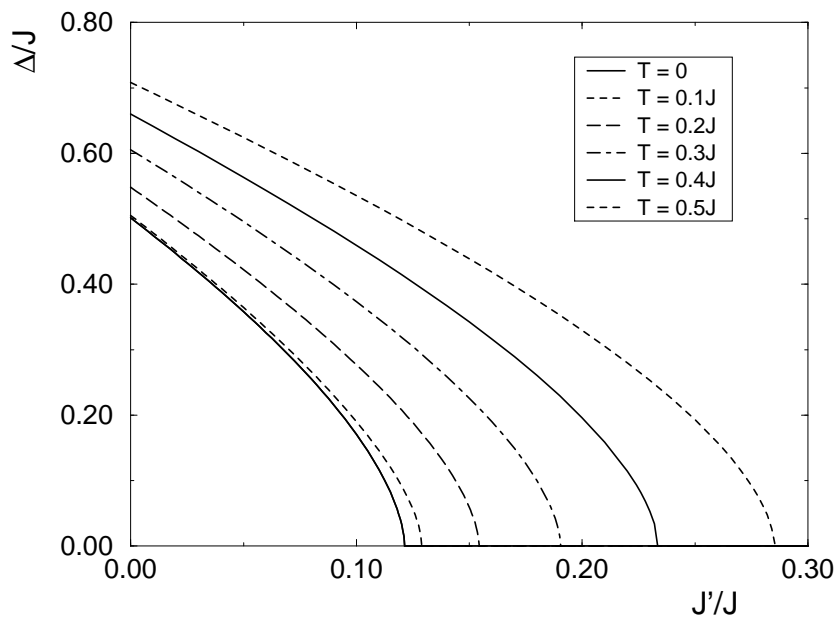


Fig. 3, B. Normand and T. M. Rice

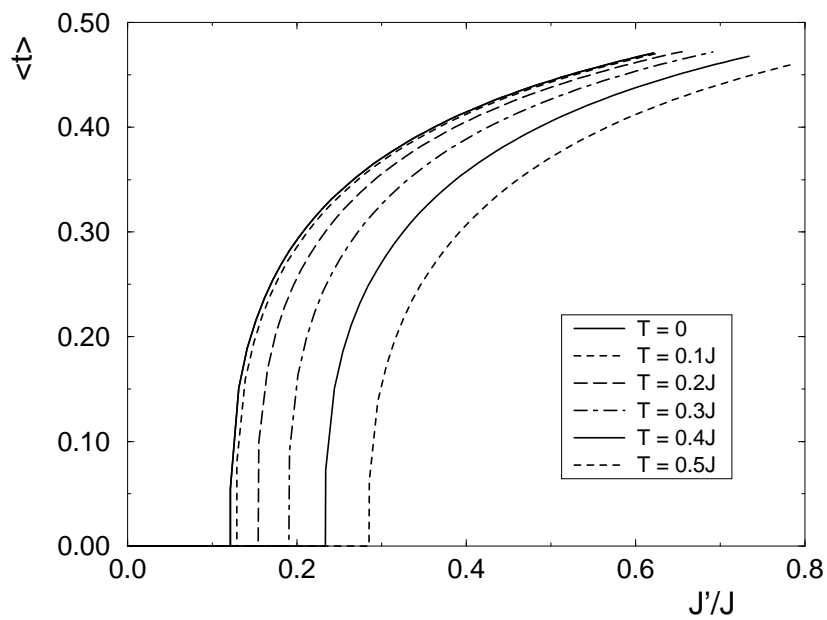


Fig. 4, B. Normand and T. M. Rice

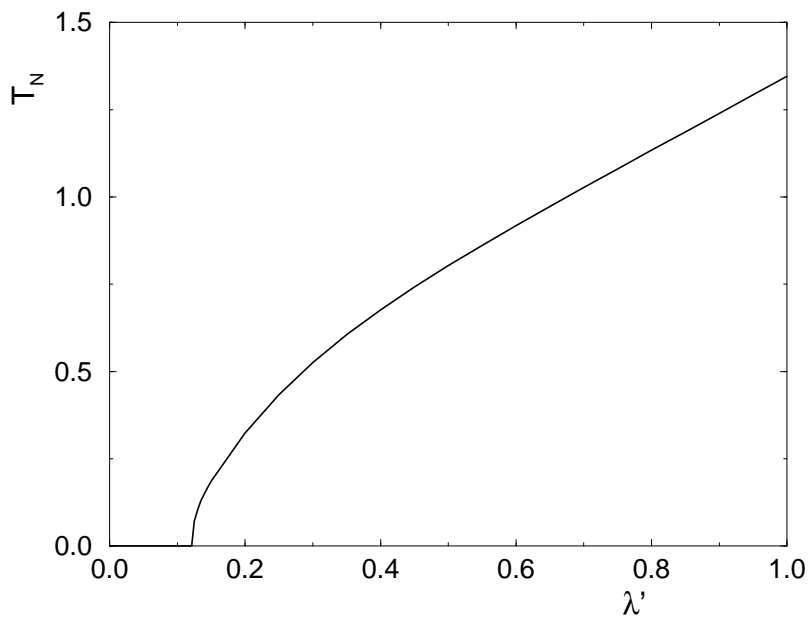


Fig. 5, B. Normand and T. M. Rice

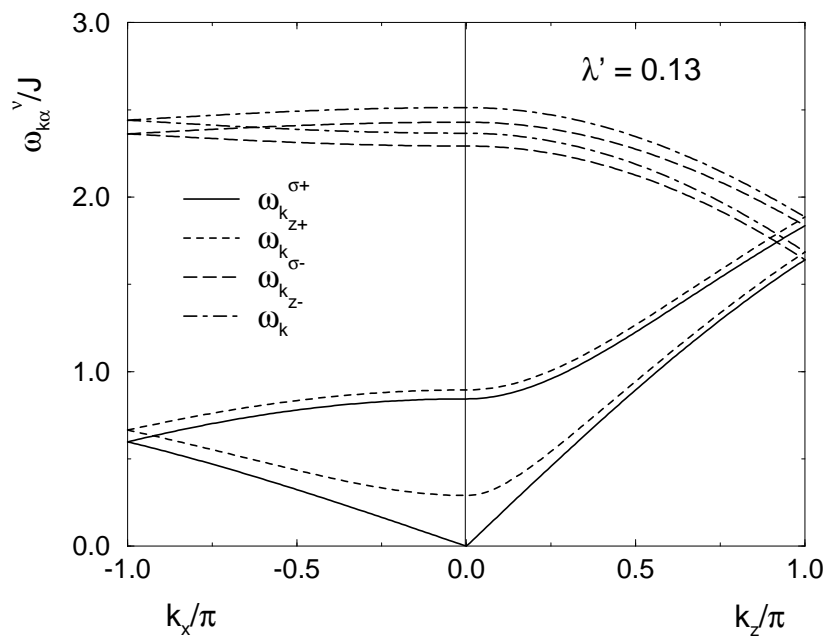
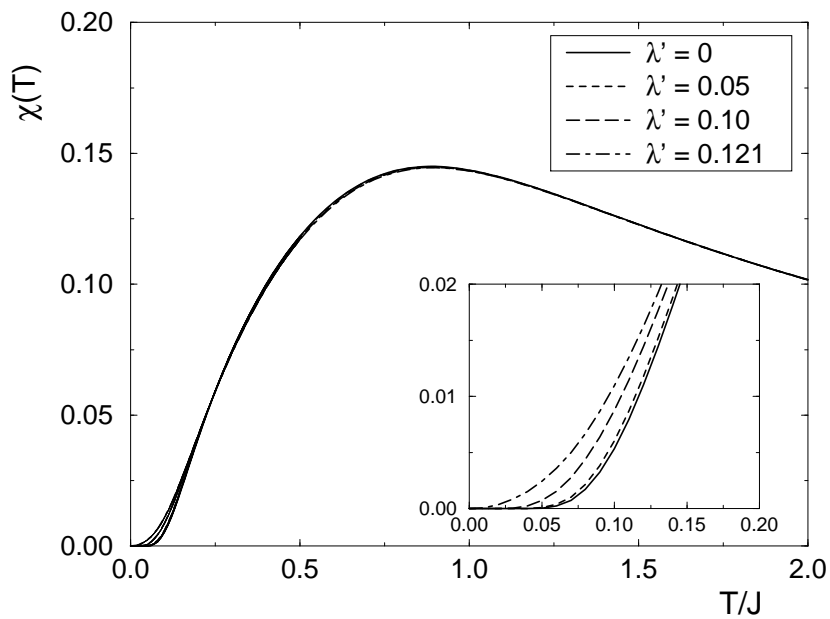
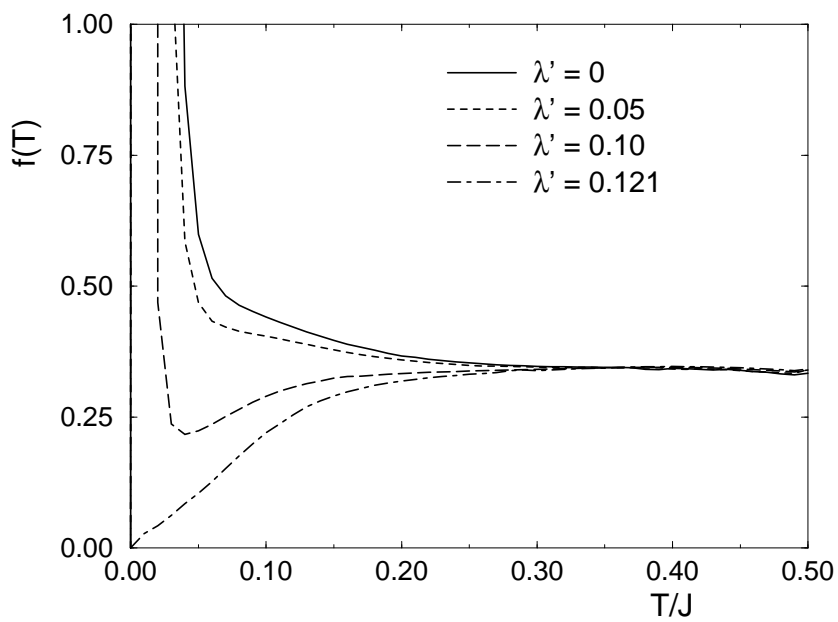


Fig. 6, B. Normand and T. M. Rice





(a)



(b)

Fig. 7, B. Normand and T. M. Rice

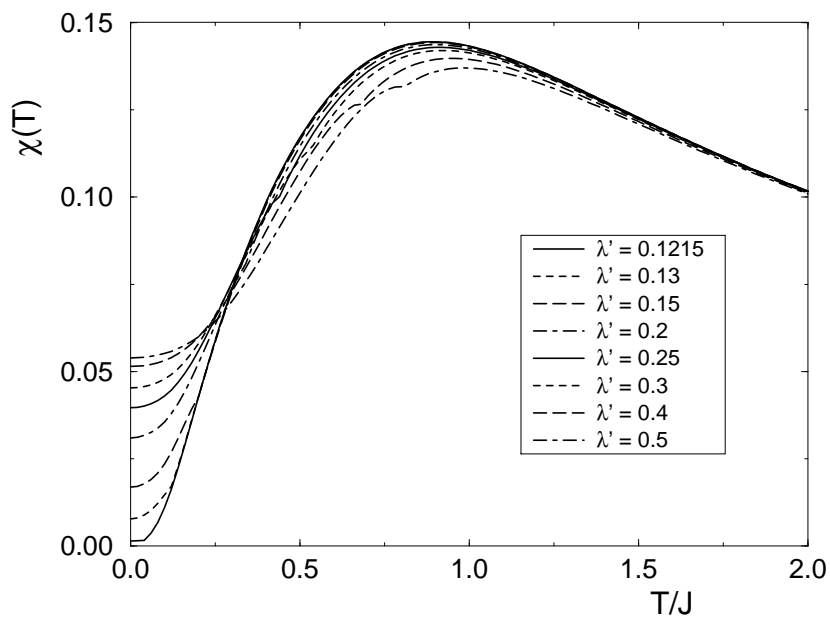


Fig. 8, B. Normand and T. M. Rice

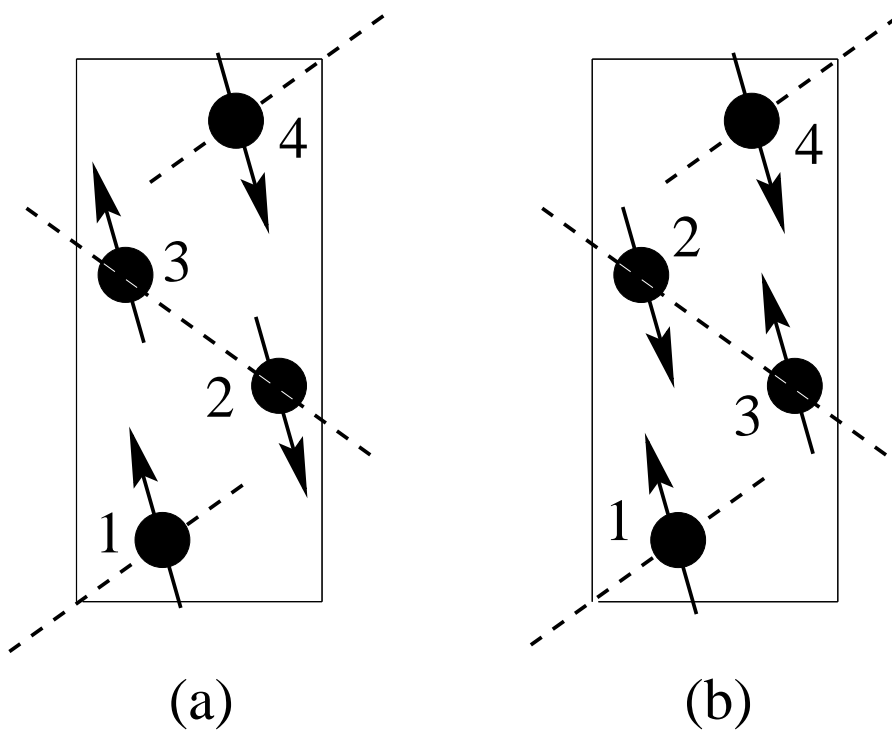
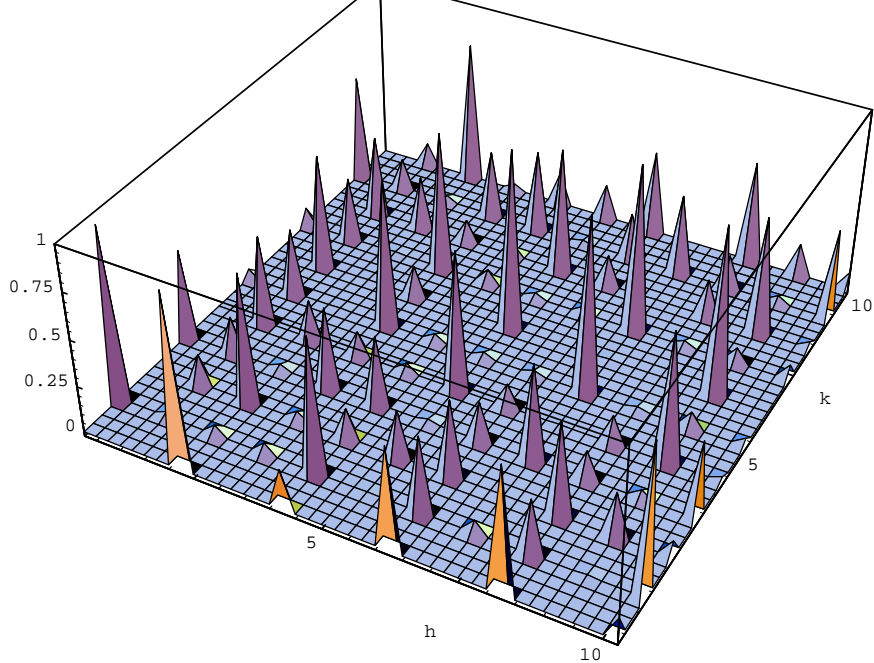
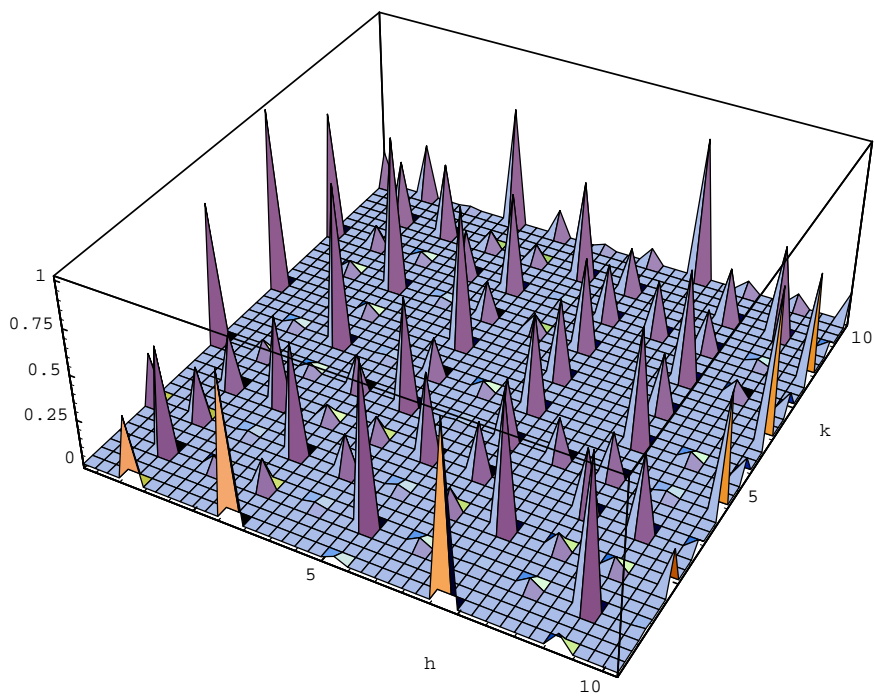


Fig. 9, B. Normand and T. M. Rice



(a)



(b)

Fig. 10, B. Normand and T. M. Rice